Fine structure of the red giant clump from *Hipparcos* data, and distance determinations based on its mean magnitude*

Léo Girardi[1], Martin A. T. Groenewegen[1], Achim Weiss[1], and Maurizio Salaris[2,1]

[1] Max-Planck-Institut für Astrophysik, Karl-Schwarzschild-Straße 1, D-87540 Garching bei München, Germany
[2] Astrophysics Research Institute, Liverpool John Moores University, Byrom Street, Liverpool L3 3AF, UK

submitted to Monthly Notices of the Royal Astronomical Society

* Based on data from the ESA *Hipparcos* astrometry satellite.

Abstract. The I-band brightness M_I of clump stars is a possible distance indicator for stellar populations. Investigations have shown that M_I is almost insensitive to the $(V-I)$ colour within the clump. Based on this, it was assumed that M_I was insensitive to age and composition of the stellar population and therefore an ideal standard candle, which could be calibrated with local clump stars, whose absolute brightness is known from *Hipparcos* parallaxes. This resulted in a distance to the LMC about 15% shorter than usually determined.
In the present paper we show that with a population synthesis approach we can reproduce the constancy of M_I with colour for the local *Hipparcos* clump sample. Nevertheless, M_I is not a constant among different populations, but depends on metallicity. As a result, the determined distance modulus to the LMC of 18.28 ± 0.18 mag is in better agreement with standard values. This resolves, at least partially, the controversial result obtained by the assumption of a universal value for M_I.
Particularly remarkable is our prediction that stars slightly heavier than the maximum mass for developing degenerate He cores, $M_{\rm Hef}$, should define a secondary, clumpy structure, about 0.3 mag below the bluest extremity of the red clump. Both features are well separated in the M_I vs. $V-I$ diagram of metal-rich stellar populations. Indeed, this secondary clump can be clearly identified in the *Hipparcos* database of stars with reliable I photometry and parallax errors smaller than 10%. Since the stars in this feature should represent a narrow range of masses, their mass determination, e.g. by the use of binary systems, can provide information about the efficiency of convective overshooting from stellar cores.
Our investigation demonstrates that the RGB clump cannot be used as a distance indicator without proper knowledge and modelling of the population under investigation. In addition, there remain unsolved problems in the models, such as correct bolometric corrections and colour transformations.

Key words: stars: evolution – Hertzsprung-Russell (HR) diagram – solar neighbourhood – Galaxy: stellar content – galaxies: distances and redshifts – Magellanic Clouds

1. Introduction

The red giant clump is an easily recognizable feature in many colour-magnitude diagrams (CMD). It consists of stars of rather low mass, which are currently undergoing their central helium burning. Physically, it is identical to the horizontal branch in globular clusters made up by less massive and more metal-poor stars.

Paczyński & Stanek (1998) recently determined the mean absolute brightness (M_I) of local clump stars making use of *Hipparcos* parallaxes. They selected the stars from the *Hipparcos* catalogue (ESA 1997) with parallax measured to better than 10%. Then they determined the mean M_I magnitude of the clump stars, $M_I^{\rm max} = -0.185 \pm 0.016$, by fitting a gaussian-like curve to the magnitude distribution of 657 stars inside the box defined by $0.8 < (V-I) < 1.25$, $1.1 > M_I > -1.4$. Selecting stars in two colour subintervals, $0.8 < (V-I) < 1.0$ and $1.0 < (V-I) < 1.25$, they found values of $M_I^{\rm max}$ formally indistinguishable from the mean. The same independence of the apparent I-band brightness $I^{\rm max}$ in the $V-I$ colour was also found for the clump stars in Baade's Window, over the entire $0.8 < (V-I) < 1.4$ interval. Based on these results, Paczyński & Stanek (1998) assumed $M_I^{\rm max}$ to be independent of the properties of the observed stellar populations, at least for stars with $0.8 < (V-I) < 1.25$. Under this assumption, the galactocentric distance was determined by comparing the apparent I magnitude of Baade's Window clump stars, $I^{\rm max}$, with the reference value obtained from the *Hipparcos* sample. The same process was repeated for stars in M31 (Stanek & Garnavich 1998), the Magellanic Clouds (Udalski et al. 1998), and the LMC alone (Stanek, Zaritski & Harris 1998). In all these cases, the mean $I^{\rm max}$ value was found to be nearly independent of the $V-I$ colour sampled.

For both the bulge and M31, the distances obtained were essentially in agreement with those obtained from other methods. In the case of the Magellanic Clouds, however, distances turned out to be significantly shorter than those derived by Cepheid stars and commonly accepted: Udalski et al. (1998) and Stanek, Zaritsky & Harris (1998) find that the relatively well-settled distance modulus of the LMC of about $(m-M)_0 = 18.5$ mag could be overestimated by 0.45 mag, or a factor of about 15% in distance, with respect to the real one. Since clump stars provide a one-step distance, this lead them to claim that *other* distance indicators (such as Cepheids) were erroneous and should be re-investigated.

Since Magellanic Cloud stars have mean metallicities well below those of local stars and of stars that define the clump in the bulge and in M31 over the $0.8 < (V-I) < 1.25$ interval, the suspicion that metallicity effects may be causing the discrepant results, is obvious. According to the above authors, theoretical models show weak dependence of $M_{\rm bol}$ and M_I (for clump stars) on either age or chemical composition. That is a surprising statement, since models in the literature (e.g. Sweigart & Gross 1976; Seidel, Demarque & Weinberg 1987; Bertelli et al. 1994, and references therein) show that clump stars of different masses and metallicities may have luminosities differing of up to 0.5 mag (see Section 2). The main support for using $M_I^{\rm max}$ as a standard candle comes, instead, from the observed independence of $M_I^{\rm max}$ on $V-I$ (and hence supposedly metallicity).

Cole (1998) accordingly proposed a revision of the clump distance to the LMC, based on the mean age and metallicity differences between the LMC and local stars. Considering these differences, and making use of the (theoretical) dependence of clump magnitude on both parameters, he shows that the LMC red clump should be about 0.32 mag brighter than the local disk one, and obtains a distance modulus of 18.36 ± 0.17 mag to the LMC. Beaulieu & Sackett (1998) obtained a good model for the LMC clump by adopting a distance modulus of 18.3 from isochrone fitting.

However, this kind of first-order explanation seems to be in contrast with the observation that $M_I^{\rm max}$ is almost constant at different $V-I$ colours in different stellar systems. Since the clump colour is usually considered as indicative of metallicity, the $M_I^{\rm max}$ constancy with colour strongly suggests that it is, in reality, inpedendent of metallicity. The question arises if theoretical models can explain this constancy in a composite stellar population, but simultaneously predict brighter clumps at lower metallicities, as required to obtain the usual LMC distance. That is one of the questions we are going to address in the following.

In this work, we intend to examine the fundamentals of the red clump method, with the aid of evolutionary models and isochrone calculations which should represent, as far as possible, the standard theoretical predictions for the behaviour of clump stars in stellar populations of different ages and metallicities. In Section 2 we briefly describe the theoretical stellar models and isochrones we used, and the general predictions for the M_I magnitude and colours of the clump stars; in Section 3 we show that the models predict a fine structure of the red clump, which is indeed observed in the M_I vs. $V-I$ diagram from *Hipparcos* data. In the light of these results, in Section 4 we show how the mean M_I for a composite stellar population can be, at the same time, almost independent of the $V-I$ colour sampled, and dependent on the mean metallicity of the population observed (being in general brighter for lower metallicities); this behaviour, together with our present knowledge on the star formation history of the LMC, helps to put the distance modulus of this galaxy closer to the more traditional value of about 18.5 mag (Section 5). Finally, in Section 6 we comment on the accuracy in distance determinations that can be obtained from the red clump method.

2. Theoretical models for clump stars

Stellar evolution theory predicts a fundamental dichotomy between the evolutionary behaviour of stars which do, and those which do not, develop electron degenerate cores after central hydrogen exhaustion. Stars of masses lower than about 2 $M_\odot$ develop degenerate cores, and climb the red giant branch (RGB) until the core mass grows to about 0.45 $M_\odot$. Then a relatively strong He-flash event lifts degeneracy, and the star settles on the core He-burning phase. The maximum mass of stars that follow this evolutionary scheme is usually denoted as $M_{\rm Hef}$ (e.g. Renzini & Buzzoni 1986; Maeder & Meynet 1989; Chiosi, Bertelli & Bressan 1992). Stars of masses slightly above $M_{\rm Hef}$ have a weakly-degenerate core, and are able to ignite helium with a lower core mass, of about 0.33 $M_\odot$; therefore their RGB phase is significantly abbreviated. For stars of higher masses, the core mass at He ignition becomes an increasing function of stellar mass, and the evolutionary phase equivalent to the RGB is practically missing. This difference in the core mass reflects directly on the luminosity of the core He-burning stars: for $M < M_{\rm Hef}$ their luminosity is almost constant at $\log(L/L_\odot) \sim 1.5$, which gives origin to the clump of red giant stars (or to the horizontal branch in the case of Pop. II stars); for masses slightly above $M_{\rm Hef}$ this luminosity is predicted to have a minimum value, about 0.4 mag below the clump of lower mass stars; and for still higher total mass the He burning stars shift progressively to higher luminosities, so that they do not correspond to the 'red clump' anymore. The exact values of the stellar masses and luminosities depend slightly on the assumed values of Z and Y. The limiting mass $M_{\rm Hef}$ also depends on the extent of convective cores during the main sequence (MS) phase: for solar composition models and adopting the classical Schwarzschild criterion for convective instability, one finds $M_{\rm Hef} \simeq 2.4\ M_\odot$ (e.g. Sweigart et al. 1990; Girardi et al. 1998), while values as low as 1.7 $M_\odot$ are found when overshooting schemes are adopted (see e.g. Maeder & Meynet 1989; Bertelli, Bressan & Chiosi 1985; Chiosi et al. 1992).

2.1. The present stellar tracks

We illustrate here the expected location of clump stars in both the theoretical, $\log(L/L_\odot)$ vs. $\log T_{\rm eff}$, and observational, M_I vs. $V-I$, planes, for a particular set of stellar models.

We use a large set of evolutionary tracks (Girardi & Bertelli 1998; Girardi et al. 1998), with metallicities ranging from $Z = 0.001$ to $Z = 0.03$ and with the helium content given by the relation $Y = 0.23 + 2.25\,Z$. This relation reproduces the initial solar helium content of 0.273 (Girardi et al. 1996) for the primordial value of $Y = 0.230$ (Torres-Peimbert, Peimbert & Fierro 1989; Olive & Steigman 1995). The typical mass resolution for low-mass stars (i.e. those with $M < M_{\rm Hef}$) is 0.1 $M_\odot$, increasing to 0.2 to 0.5 $M_\odot$ for intermediate-mass stars (i.e. $M > M_{\rm Hef}$). The $Z = 0.019$ models, for instance, were computed for masses 0.5, 0.55, 0.6, 0.7, 0.8, 0.9, 1, 1.1, 1.2, 1.3, 1.4, 1.5, 1.6, 1.7, 1.8, 1.9, 1.95, 2, 2.2, 2.5, 3, 3.5 $M_\odot$. We used an updated version of the Padova code (see Bertelli et al. 1994, and references therein), with the input physics as described in Girardi et al. (1996) and Girardi & Bertelli (1998). We assume moderate convective overshooting (see e.g. Chiosi et al. 1992 for a review), so that we find $M_{\rm Hef} = 2.0\ M_\odot$ for our $Z = 0.019$ tracks.

For $M < M_{\rm Hef}$, the RGB evolutionary sequences are stopped at the He-flash, and continued from a quiescent He-burning model with the same core mass and chemical structure as the last RGB model. Therefore, all the relevant evolutionary phases previous to the onset of the thermally-pulsing regime of the asymptotic giant branch (AGB) are included in the tracks. Models are computed at constant mass, since the effect of mass loss can be realistically considered during the preparation of isochrones (see e.g. Renzini 1977; Bertelli et al. 1994).

The upper panel of Fig. 1 shows the location of the zero-age horizontal branch (ZAHB) for $M \geq 0.7\ M_\odot$ in the HR diagram. We understand the ZAHB in this context as the location of stars beginning their central helium burning phase, independent of initial stellar mass. It is essentially defined by the lowest luminosity reached by our He-burning tracks, so that the depicted lines can be thought as the lower envelope of clump stars in the HR diagram, as a function of mass and metallicity. ZAHB models with masses between 0.7 and $M_{\rm Hef}$ describe a kind of hook or semi-circle in the diagram, which is limited to a small range of luminosities [e.g. $1.5 \lesssim \log(L/L_\odot) \lesssim 1.7$ for $Z = 0.019$]. It reflects the small range of core masses for these stars at the moment of He-ignition. At the hottest extremity of this hook, the models with $M > M_{\rm Hef}$ depart to high luminosities: these are the stellar models in which He burning started under non-degenerate conditions.

The precise shape of the ZAHB in the HR diagram is determined by the interplay of several factors, mainly related to the properties of the stellar envelopes (e.g. its total mass, Y and Z), and to the core mass for those stars close and above $M_{\rm Hef}$. The general behaviour is that stars with lower masses ($M \lesssim 1\ M_\odot$) or with $M \simeq M_{\rm Hef}$ have lower luminosities than stars with $M \simeq 1.4\ M_\odot$, and that in this mass range higher masses correspond to higher temperatures. For lower metallicities and at the extreme of lower masses ($M \lesssim 0.7\ M_\odot$), stars also develop higher temperatures, going rapidly to the region of the blue HBs (eventually closing the ZAHB line in the HR diagram, and

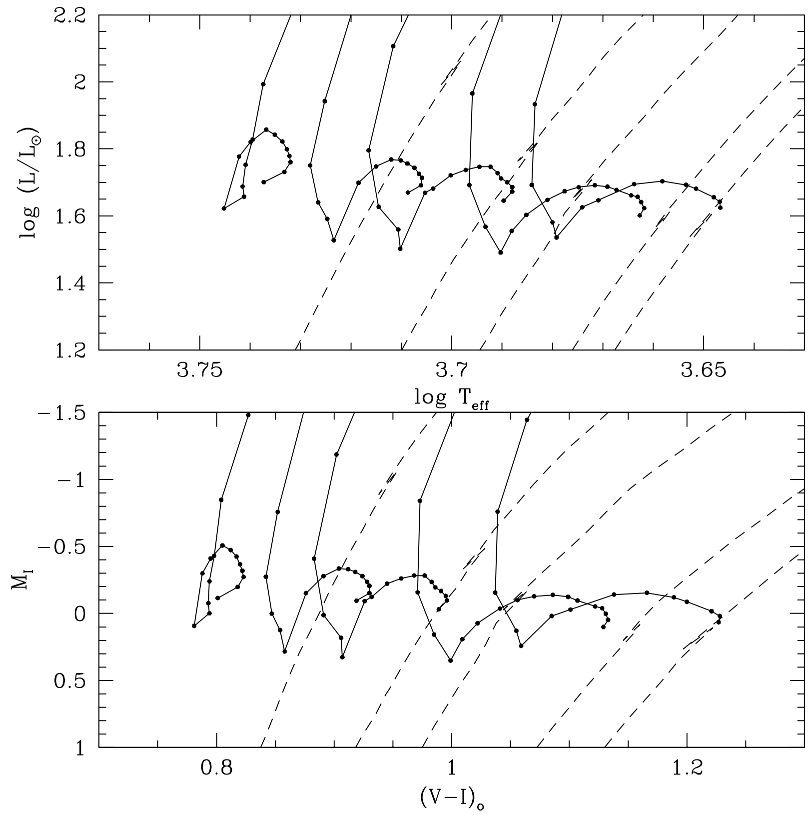

Fig. 1. Position of the ZAHB (onset of quiescent He-burning) for stellar evolutionary tracks of different masses and metallicities, in the HR (top panel) and M_I vs. $V-I$ (bottom panel) diagrams. Dots represent the computed models, at typical mass intervals of 0.1 $M_\odot$ for $M \lesssim 2\ M_\odot$, and 0.2 to 0.5 $M_\odot$ for $M \gtrsim 2\ M_\odot$. For the sake of clarity, only models with $M > 0.7\ M_\odot$ are plotted. Metallicities are, from left to right, $Z = 0.001$, 0.004, 0.008, 0.019 and 0.03. The dashed lines correspond to the RGBs of 4 Gyr isochrones with the same values of metallicity.

crossing the RR Lyrae instability strip; see e.g. the behaviour of $Z = 0.001$ models in Fig. 1). The lower panel of Fig. 1 shows the theoretical results transformed into the observed M_I-$(V-I)_0$ plane (see Section 3.1).

It is convenient to limit our discussion to only those stars which can be relevant in defining the red clump morphology. Only $Z \gtrsim 0.004$ models, for instance, can produce red clumps in the $V-I$ colour range under discussion (see Fig. 1). Moreover, $Z \gtrsim 0.004$ stars with ZAHB masses lower than about 0.8 $M_\odot$ are hardly present in the stellar populations we will consider, since they (i) neither live long enough for reaching the He-burning phase during a Hubble time, (ii) nor are produced by mass loss on the RGB of more massive stars, if we assume that Reimers' (1975) mass loss prescription is valid. Therefore we can further limit the analysis to stars with $M \gtrsim 0.8\ M_\odot$. What turns out is that, for a single value of Z, clump stars of relatively high masses (and hence younger) are systematically hotter than those of lower masses (and hence older). Moreover, the bluest are also the faintest among the clump stars.

2.2. Mass distribution of clump stars

When we deal with composite stellar populations, it is also important to consider what is the relative probability of populating each section of the clump. This can be estimated from the following:

First, if we neglect mass loss on the RGB, we have that at any age clump stars have masses $M_{\rm cl}$ similar to turn-off ones, i.e. $M_{\rm TO} = M_{\rm cl}$. The probability of having ZAHB masses in the interval $[M_{\rm cl}, M_{\rm cl} + {\rm d}M_{\rm cl}]$ is then proportional to the product of the initial mass function (IMF) ϕ_M with the star formation rate at the time the stars formed, $\psi(T-t)$, where T is the galactic age. For our $Z=0.019$ models, TO-ages are related to masses according to

$$\log(t/\mathrm{yr}) \simeq 10.14 - 3.25 \log(M_{\mathrm{TO}}/M_\odot) \,. \quad (1)$$

Core He-burning stars evolve from the ZAHB to higher luminosities leaving the clump after a time interval t_{He}. They grow in luminosity by only about $0.05-0.1$ mag, before the faster evolution towards the early-AGB starts. Therefore, the resulting probability of detecting a star of mass M_{cl} in the clump is proportional to $\phi_M(M_{\mathrm{cl}})\,\psi[T-t(M_{\mathrm{cl}})]\,t_{\mathrm{He}}(M_{\mathrm{cl}})$. The function t_{He} assumes almost constant values, close to 10^8 yr, for the entire range $M_{\mathrm{cl}} \lesssim M_{\mathrm{Hef}}$, but nearly doubles for masses slightly above this limit (Girardi & Bertelli 1998).

Thus, in the case of constant star formation, the mass distribution of clump stars closely follows the IMF, except for those stars with mass slightly higher than M_{Hef}, the detection of which would be favoured by a factor of two with respect to this rule. For instance, if we assume $\psi(t)$ constant in the solar neighbourhood from 1 to 10 Gyr (corresponding to M_{cl} from 2.2 to about 1 $M_\odot$), the local sample of stars would contain only 2.5 times less clump stars with mass in the interval $2.1 > (M_{\mathrm{cl}}/M_\odot) > 2.0$ than in the $1.1 > (M_{\mathrm{cl}}/M_\odot) > 1.0$ one.

Mass loss on the RGB causes stars of a given age to have lower values of M_{cl} than given by equation (1) under the assumption that $M_{\mathrm{TO}} = M_{\mathrm{cl}}$. However, the effect is not dramatic. If we adopt Reimers' (1975) mass loss rates with an efficiency parameter $\eta = 0.4$ (Renzini & Fusi Pecci 1988, and references therein), we conclude that only the long-lived stars with initial masses $M \lesssim 1.2\ M_\odot$ have their masses reduced by more than $0.1\ M_\odot$. Stars of masses higher than about 1.5 $M_\odot$ are virtually unaffected. Therefore, mass loss causes a spread of the stars in the red extremity of the clump to slightly lower masses and hence luminosities (see Fig. 1), while the bluest part of the clump remains essentially the same.

3. Clump distribution in the M_I vs. $V-I$ plane

3.1. Theoretical predictions

All effects described above, which determine the observed distribution of clump stars in the HR diagram of composite stellar populations, can be simulated by means of evolutionary population synthesis models. The code we have for this purpose (see Girardi & Bertelli 1998) is based on the construction of isochrones for different ages and metallicities (interpolations in both parameters are allowed), which are then populated with stars and summed up in order to produce the theoretical colour-magnitude diagrams (CMD) and luminosity functions (LF). Mass loss along the RGB is taken into account during the stage of isochrone construction, and given by the Reimers' (1975) formula multiplied by a factor $\eta = 0.4$. Every point in the isochrones is transformed to the observational colours and magnitudes according to the Kurucz (1992) transformations. The latter produce some systematic shifts in the transformed colours, which have so far been well documented (e.g. Worthey 1994; Gratton, Carretta & Castelli 1996; Charlot, Worthey & Bressan 1996). Fortunately, the inadequacies in Kurucz transformations are not critical in the $V-I$ colour, being smaller than 0.1 mag for both dwarfs and giants of solar metallicity (Gratton et al. 1996).

Fig. 2 shows the result of the simulations in the M_I vs. $V-I$ diagram. Illustrated in the top panel is the result of summing up stellar populations with ages from 0.1 to 10 Gyr (younger stellar populations certainly do not contribute to the clump), with mean solar metallicity ($Z=0.019$) and a metallicity dispersion of only $\sigma(\log Z) = 0.1$. It is meant to represent, as a first approximation, the bulk of local stars sampled by *Hipparcos*. No attempt was made to simulate dispersions in reddening and distance, observational errors, and the presence of multiple stars. Any age-metallicity relation was also ignored in this first simulation. In order to obtain more realistic models, we make a second simulation, this time assuming that the metallicity decreases with age at a rate of -0.07 dex/Gyr (Carraro, Ng & Portinari 1998), and correcting for the relative number of stars with different scale heights above the galactic plane, according to the $f(Z)$ function indicated by the $[\epsilon = 0.02, P = 1.8]$ case in Sommer-Larsen (1991). The result is presented in the bottom panel of Fig. 2.

In both cases, the theoretical clump presents a main almost-horizontal feature, ranging from $V-I = 1.0$ to $V-I = 1.1-1.2$, and a secondary, predominantly vertical feature, developing at the extreme left of the clump. This secondary structure is caused by the stars with masses above $M_{\mathrm{Hef}} \simeq 2\ M_\odot$, and its maximum density occurs ~ 0.3 mag *below* the main body of the clump. Also, it originates a kind of plume departing from the clump to higher luminosities. The horizontal part appears to be a generic feature of the local clump.

3.2. The clump from Hipparcos *data*

From the *Hipparcos* database we have selected stars that fulfilled the following criteria: error in parallax $< 10\%$, a parallax > 0, the 'data-points-rejected' (DPR, field H29) flag $< 10\%$, 'goodness-of-fit' (GOF, field H30) flag < 3, the

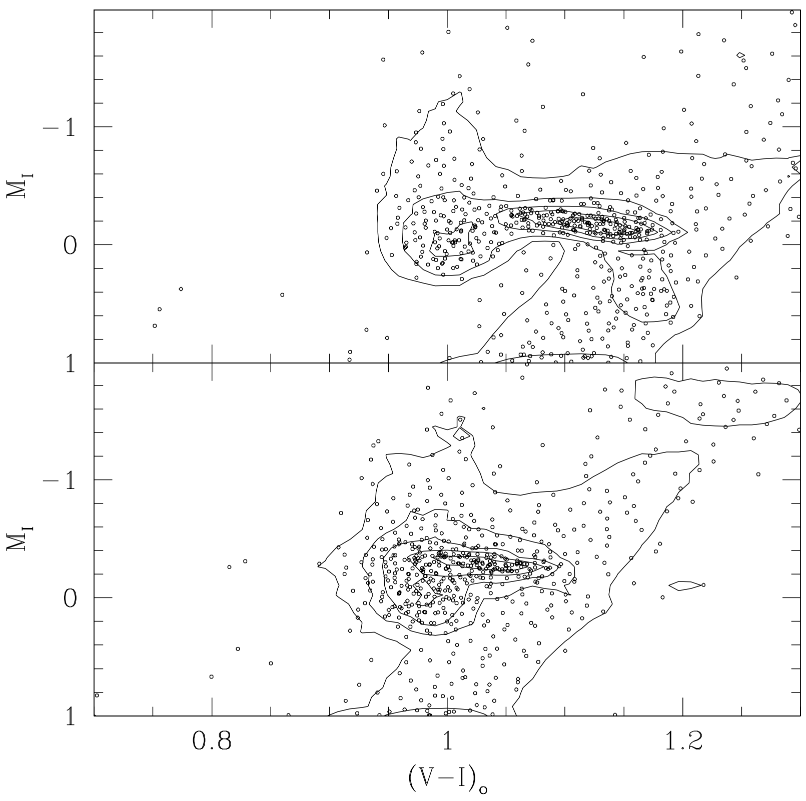

Fig. 2. Theoretical distribution of clump stars in the M_I vs. $V-I$ diagram. We simulate a total of 600 stars (dots) following the predicted density distributions. 5 countour levels (continuous lines) delimit regions with the same density of stars. This model is for a composite stellar population with constant star formation rate in the interval $0.1 < (t/\mathrm{Gyr}) < 10$ and mean solar metallicity (upper panel), and for another one with constant star formation but assuming an age metallicity relation and larger scale heights for older stars (see text for details).

'number of components' (field H58 in the database) equal to 1, and the 'source for I photometry' flag (field H42) either A, C, E, F or G. This results in 2546 stars. These are the same selection criteria as Paczyński & Stanek (1998), except that we added the criteria on DPR, GOF and field H58 to eliminate bad solutions and to a large extent binary stars. The red clump derived from these data is plotted in Fig. 3, and limited to samples with parallax errors smaller than 5% (upper panel) and 10% (lower panel). Therefore, absolute magnitudes for these two samples are known to better than 0.11 and 0.22 mag (standard errors), respectively. The $V-I$ colours are also expected to be accurate to within 0.05 mag, since reddening is negligible for them; the mean error in $V-I$ for this dataset is of order 0.02 mag.

Several aspects of the observed red clump in Fig. 3 find some correspondence with the structure of the theoretical one, shown in Fig. 2. In particular, it is clear that the observed stars are more spread in M_I at the blue side of the clump than at the red. Also, there is a locally higher concentration of stars at $[M_I \simeq 0.0, V-I \simeq 0.92]$, which is more evident in the plot which considers data with parallax errors smaller than 5%. Also, a plume of brighter stars is present at $V-I \simeq 0.9$, going from $M_I \simeq -0.5$ to about -1.0. These latter features nicely correspond to those predicted to occur at the blue side of the clump.

However, it is also evident that the theoretical distribution is systematically shifted to redder colours with respect to the observed one. In order to make both coincide, a shift of about $\Delta(V-I) = -0.08$ to the models is required; that is of the same order of the inadequacies found to date in the $V-I$ colour transformations of Kurucz (1992).

The plume departing from the clump to higher luminosities has been already noticed by Beaulieu & Sackett (1998) in BV data from the *Hipparcos* database, and an equivalent feature in the CMD of the LMC has been at the center

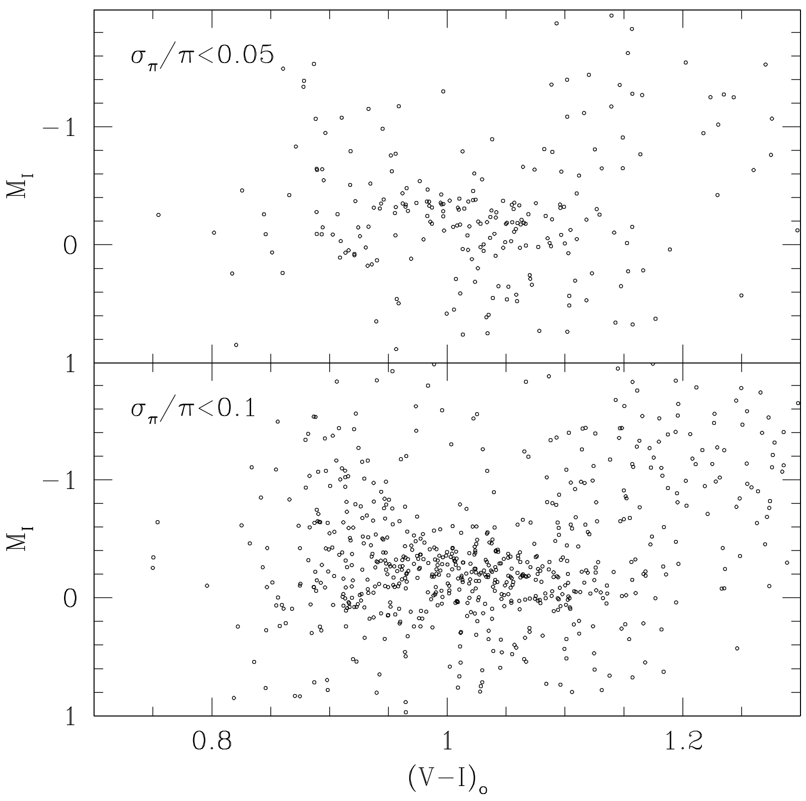

Fig. 3. Distribution of clump stars in the M_I vs. $V-I$ diagram, from *Hipparcos* data. The sample is limited to data with parallax errors smaller than 5% (upper panel) and 10% (lower one). In order to suppress artificial superposition of points in the diagram (due to limited digits in the database), random numbers between -0.005 and 0.005 were added to the $V-I$ colour.

of a recent debate about its origin (Zaritsky & Lin 1997; Beaulieu & Sackett 1998). The structure located slightly below the main red clump, at its bluest extremity, passed however unnoticed even in works which dealed with the clump morphology from *Hipparcos* data (e.g. Jimenez et al. 1998). Before going ahead, it is important to be sure of the reality of this kind of 'secondary clump'.

In Fig. 4, we show how the red clump shows up in the M_V vs. $B-V$ diagram, as predicted by the model which does not consider the age-metallicity relation (upper panel), and as observed by *Hipparcos* (lower panel, sample limited to 5% parallax errors). Notice that also in this plot models are systematically redder by about $\Delta(B-V)=0.08$ with respect to observations. In the lower diagram, we identify by crosses the stars which were located in the small box with $0.84<(V-I)<0.94$ and $0.2>M_I>-0.2$ in the previous Fig. 3. It can be noticed that the red clump is expected to be less resolved in this diagram. In addition it is inclined, due to the stronger dependency of bolometric corrections on the $B-V$ colour. Nonetheless, the stars that define the secondary clump in Fig. 3 again occupy a well-defined region of the M_V vs. $B-V$ diagram, being located to the blue and to a higher magnitude (i.e. are fainter) with respect to the main body of the red clump at that colour. The statistics provided in this plot is higher than that derived from the equivalent one in Fig. 3.

We conclude that the predition of the theoretical models for the secondary clump appears to be realistic, since the substructure is observed in both CMD diagrams, and it is unlikely that it might be caused by such effects as reddening, bad number statistics, contamination from the RGB and low-metallicity clump stars, photometric and parallax errors.

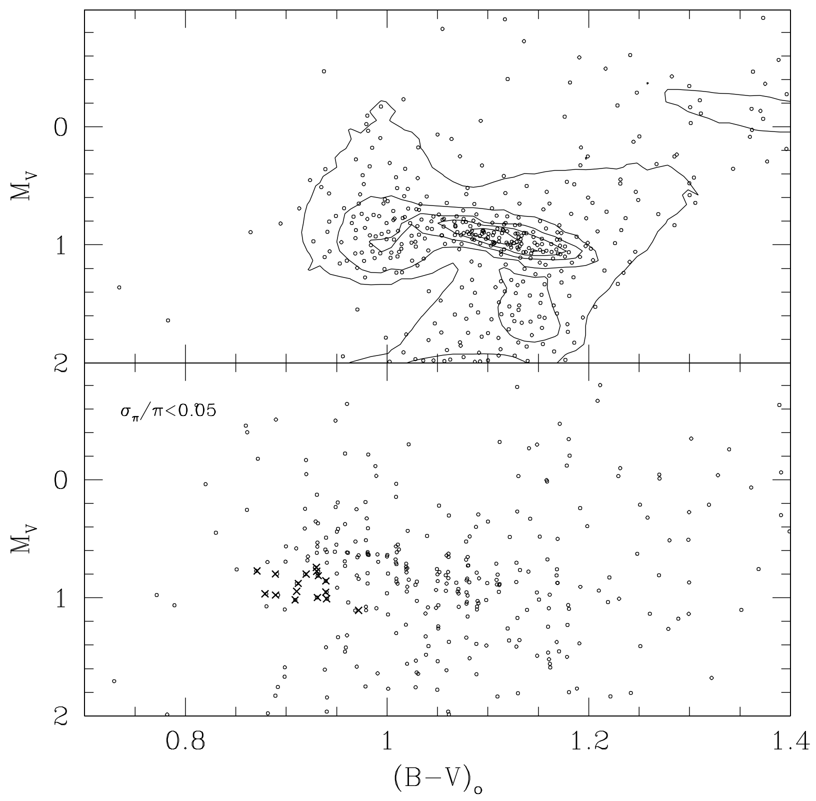

Fig. 4. Distribution of clump stars in the M_V vs. $B-V$ diagram, from theoretical models (upper panel; corresponding to the model illustrated in the upper panel of Fig. 2, for a total number of 400 stars), and *Hipparcos* data with parallax errors smaller than 5% (lower panel). Stars belonging to the secondary clump in the M_I vs. $V-I$ diagram (with $0.84 < (V-I) < 0.94$ and $0.2 > M_I > -0.2$, see Fig. 3) are indicated by crosses.

There are two remarkable aspects in this feature:

1. It represents an old prediction of stellar models, that the core masses at helium ignition has a minimum value for $M \gtrsim M_{\rm Hef}$, corresponding to a minimum value of luminosity. As far as we are aware, the only observational search for this feature was carried out by Corsi et al. (1994), who successfully located a minimum in the V luminosity of clump stars for LMC clusters about 0.6 Gyr old (corresponding to 1 Gyr if moderate overshoot is assumed). In Girardi & Bertelli (1998), the present models with $Z = 0.008$ are shown to provide a good general description of Corsi et al. (1994) data in regard to this point. The presence of a similar feature in *Hipparcos* data provides further confirmation of theoretical predictions.
2. The observation of such a feature in a local, nearby sample of stars opens the possibility of further testing stellar models. As discussed in Section 2, stars in this secondary clump correspond to a quite limited interval of stellar masses, which goes from $M_{\rm Hef}$ to about $M_{\rm Hef} + 0.3\ M_\odot$. Therefore, the direct measurement of their masses could provide stringent constraints to $M_{\rm Hef}$, and therefore on the efficiency of convective core overshoot for stars of similar masses.

In order to check the latter point, we looked for binary stars in the *Hipparcos* catalog, in which the primary could be considered a member of this secondary clump. We found 7 binaries contained in the $0.84 < (V-I) < 0.94$ and $0.2 > M_I > -0.2$ box, two of which are visual ones with reliable orbital parameters in the literature:

– For HD 41116, the orbital parameters by Heintz (1986) and *Hipparcos* parallax provide a total mass of $4.30 \pm 0.66\ M_\odot$ for the system. As both primary and secondary are evolved (K0III+G8III,IV: according to Stephenson &

Sanwal 1969), their masses would be similar and of about 2.1 $M_\odot$ each. A complication arises from the later-type star being itself a spectroscopic binary (WDS catalog; Worley & Douglass 1997).
– HD 90537 is a K0III,IV+F8V binary (Edwards 1976), with a magnitude difference of 1.42 mag between both components (*Hipparcos* catalog). The orbital parameters and fractional mass given by Heintz (1982), together with *Hipparcos* parallax, indicate a mass of $1.92 \pm 0.34\ M_\odot$ for the primary, and $0.53 \pm 0.16\ M_\odot$ for the secondary. The mass of the primary is consistent with the interpretation that it should have a mass close to $M_{\rm Hef}$. However, the low value of mass obtained for the secondary seems in contradiction with its estimated spectral type, F8V.

The above numbers do not give a clear indication whether the primary stars should belong to the secondary clump we found, and whether their masses are really close to 2 $M_\odot$. In both cases, the precise classification of the component stars would be necessary in order to better constrain the characteristics of the primary. A systematic study of them would be of high interest.

4. Distance determinations by means of the red clump

In most of the works that used the red clump as a standard candle, the LF of clump stars has been modeled by fitting the function

$$N(M_I) = a + bM_I + c{M_I}^2 + \frac{N_{\rm tot}}{\sigma\sqrt{2\pi}} \exp\left[-\frac{(M_I - M_I^{\rm max})^2}{2\sigma^2}\right] . \qquad (2)$$

over a limited M_I and $V-I$ interval. The fit to *Hipparcos* data provides the reference value of $M_I^{\rm max}$. Similarly, a value of $I^{\rm max}$ can be derived for the red clump in distant stellar systems, and the distance modulus $m - M = I^{\rm max} - M_I^{\rm max}$ is obtained in a single step.

4.1. Calibrating $M_I^{\rm max}$ from Hipparcos *data*

Following Paczyński & Stanek (1998), we have modelled the *Hipparcos* data by a chi-square fit of equation (2). In order to generate solutions with acceptable chi-square residuals, fittings were limited to the $1.0 > M_I > -1.5$ interval.

Fig. 5 presents the results for the data in the $0.8 < (V-I) < 1.25$ colour interval, sampled with a 0.1 mag resolution (upper panel). We obtain for this distribution a best fit with $M_I^{\rm max} = -0.177$ and $\sigma = 0.226$. These values agree, within the errors, with those obtained by Paczyński & Stanek (1998) and Stanek & Garnavich (1998), i.e. $M_I^{\rm max} = -0.185 \pm 0.016$ and $\sigma = 0.243$, from similar data. The small differences in the numbers probably reflect the different approaches in the fitting procedures, and the small differences in the selected samples.

It is worth remarking that the sample of red clump stars here used is essentially a complete one. Indeed, stars in the clump and with parallax errors smaller than 10% are always at least 0.5 mag brighter than the $V \simeq 8.5$ completeness limit of the *Hipparcos* catalogue.

The bottom panel in Fig. 5 presents the LF for the *Hipparcos* data when corrected by the Lutz-Kelker bias according to Salaris & Groenewegen (1998). This procedure follows Turon Lacarrieu & Crézé (1977) and Smith (1987) in that it assumes one has a-priori knowledge about the absolute magnitude of the sample of stars, described by a Gaussian distribution with a mean and error. The Lutz-Kelker correction is a statistical one and therefore one can also calculate the error in the correction. This novelty is outlined in Salaris & Groenewegen (1998).

First, main-sequence stars and giants were separated. Either by the luminosity classification and the spectral type listed in the *Hipparcos* database, or on colour and absolute magnitude using the *Hipparcos* parallax as listed. A star was considered to be a dwarf if $M_I > -2.0 + 5.333\,(V-I)$, or if $M_I > 5$ and $V - I > 1.5$. For all stars considered to be dwarfs we used as theoretical input value in the Lutz-Kelker correction an empirical value for M_I as a funtion of $V-I$ colour, based on the *Hipparcos* data for stars with a parallax better than 5%. The assumed spread in the theoretical value was estimated by eye based on the spread in the data, and is 0.35 mag for $V - I < 0.75$, and 0.15 mag else. All other stars are considered to be clump giants and a mean and spread of -0.18 and 0.24 are used.

Thus, after correcting the M_I data in this way, we obtain a slightly brighter, and significantly sharper clump, with $M_I^{\rm max} = -0.209$ and $\sigma = 0.160$ (Fig. 5).

Fig. 6 instead presents LFs for the original data (without LK correction) in the $0.8 < (V-I) < 1.25$ interval (upper panel), and sampled in the two separate $1.0 < (V-I) < 1.25$ (middle panel) and $0.8 < (V-I) < 1.0$ (lower one) colour intervals, at 0.1 mag resolution. For the two cases we find $M_I^{\rm max} = -0.173$ and $\sigma = 0.201$, respectively $M_I^{\rm max} = -0.196$ and $\sigma = 0.289$. What is remarkable in these histograms is the higher dispersion σ in the blue part of the clump. This high dispersion is interpreted as the result of evolutionary effects, as discussed below.

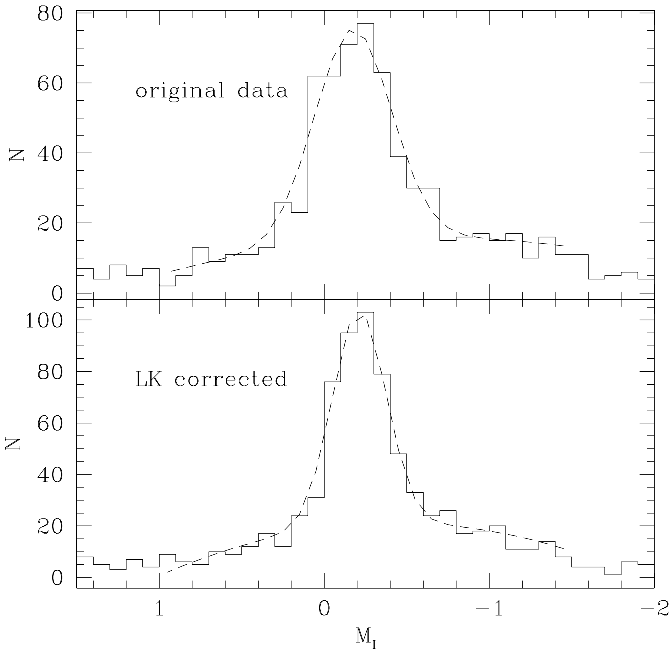

Fig. 5. LFs for clump stars in *Hipparcos* data with parallax errors smaller than 10% (continuous line: histogram of the data; dashed line: chi-square fit of equation 2). The upper panel presents the original data in the $0.8 < (V-I) < 1.25$ interval, while the lower one presents the data corrected by Lutz-Kelker bias, as discussed in the text.

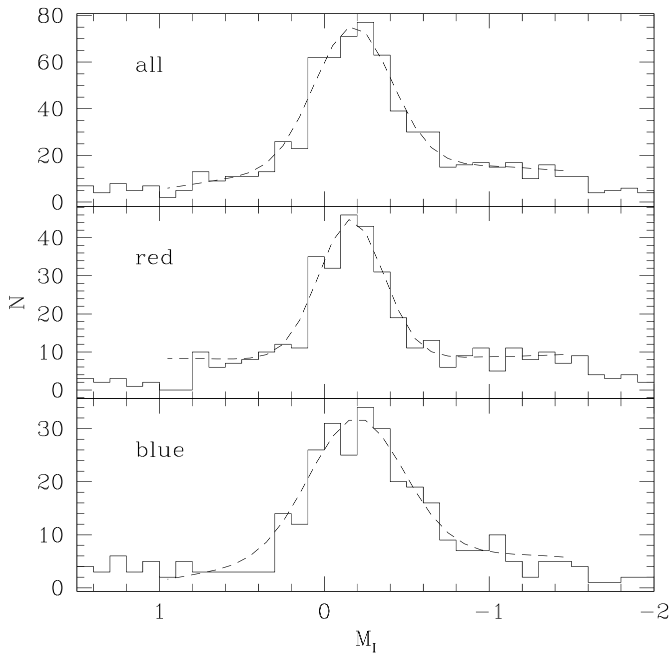

Fig. 6. LFs for clump stars in *Hipparcos* data, as in Fig. 5. We present the data in the complete $0.8 < (V-I) < 1.25$ interval (upper panel); and divided into red ($1.0 < (V-I) < 1.25$; middle) and blue ($0.8 < (V-I) < 1.0$; lower) samples.

4.2. Model predictions for $M_I^{\max}$

We are now going to discuss what, according to our models, is the expected LF of clump stars. The aim is to cast light on the factors which give origin to the observed LFs shown in Figs. 5 and 6, and which can also influence the derived values of $M_I^{\max}$. We start the comparison with the simple model depicted in the upper panel of Fig. 2, which gives a reasonable description of the clump in the M_I vs. $V-I$ diagram. However, our models are first corrected by the colour shift $\Delta(V-I) = -0.08$, otherwise the comparison with observed $M_I^{\max}$ values would be meaningless.

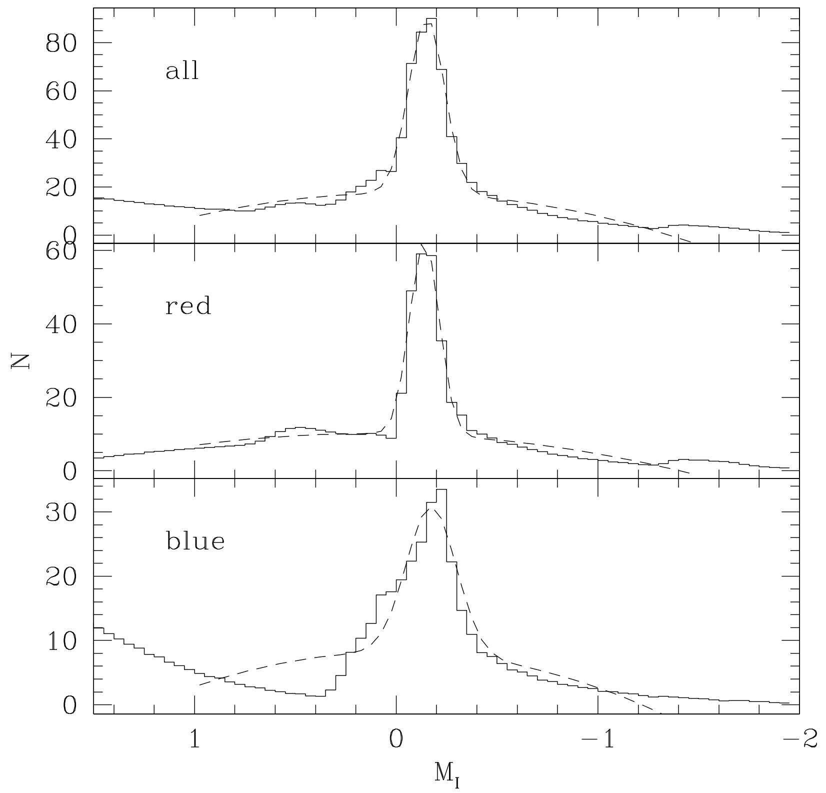

Fig. 7. Theoretical LFs for the simulation depicted in the upper panel of Fig. 2. The original simulation was, previously, shifted by $\Delta(V-I) = -0.08$, in order to reproduce the colour range appropriate to the red clump observed by *Hipparcos*, and the relative numbers of red and blue stars. Similarly to Fig. 6, we present the LFs for 3 different colour intervals: for the complete $0.8 < (V-I) < 1.25$ one (upper panel); and divided into red ($1.0 < (V-I) < 1.25$; middle) and blue ($0.8 < (V-I) < 1.0$; lower) samples. The LFs are normalized to the observed distributions (Fig. 6).

In Fig. 7, we present the synthetic M_I LF for different cases, representing all stars, and those in the red or blue parts of the clump. Again, 'blue' and 'red' parts are defined by stars in the colour intervals $0.8 < (V-I) < 1.0$ and $1.0 < (V-I) < 1.25$, respectively. We checked that the shift of $\Delta(V-I) = -0.08$ applied to the models allows us to reproduce the same relative number of blue and red clump stars as in the *Hipparcos* sample of Fig. 6.

The fit of equation (2) describes well the central spike due to clump stars, at $0 > M_I > -0.4$, but not the wings. Both wings are essentially due to evolutionary effects: the bright one, extending up to about $M_I \simeq -0.9$, is caused by stars which have evolved already from the ZAHB, while the faint one is caused mainly by the stars with $M \gtrsim M_{\rm Hef}$, located at about $0.3 > M_I > -0.1$, and appears only in the blue colour bin. In the red bin, there is another, fainter bump-like feature below the clump, at $0 > M_I > 0.6$, which corresponds to the bump of the RGB stars (see e.g. Renzini & Fusi Pecci 1988; Cassisi & Salaris 1997). Another interesting feature present in the plot is the bump in the LF caused by the presence of early-AGB stars, located at $-1.3 > M_I > -1.8$, in the red bin. The latter two features are conspicuous in CMD studies of galactic globular clusters (e.g. Fusi Pecci et al. 1990; Buonanno, Corsi & Fusi Pecci 1985).

For this theoretical simulation, we obtain $M_I^{\rm max} = -0.151$, $\sigma = 0.089$ for all stars, $M_I^{\rm max} = -0.140$, $\sigma = 0.073$ for red ones, and $M_I^{\rm max} = -0.174$, $\sigma = 0.123$ for blue ones. It is clear that the σ values obtained are about 1/3 of the observed ones (see Fig. 6). Also, blue stars have a $M_I^{\rm max}$ value -0.034 mag brighter than red ones.

The simulations cannot be simply compared to observations, since the latter include the errors in parallax and hence in distance modulus. Therefore, we have convolved the theoretical distribution of Fig. 7 with the expected distribution of errors in distance modulus resulting from the errors in *Hipparcos* parallaxes (see Appendix).

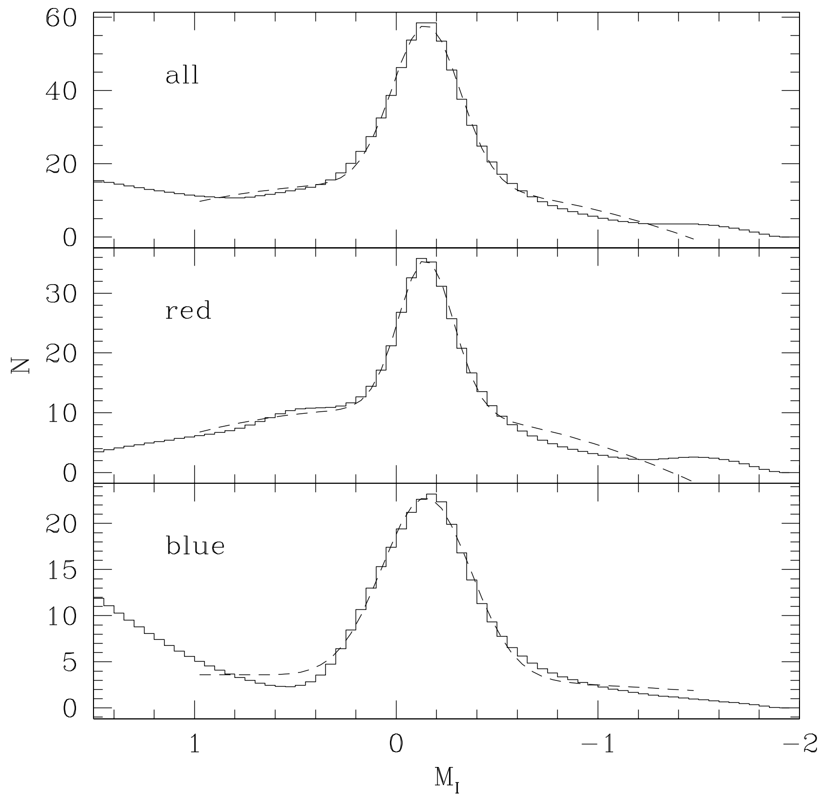

Fig. 8. LFs for the simulations depicted in Fig. 7, this time convolved with the function $f(\delta_{m-M})$ (equation (A1)) shown in Fig. 11. These LFs should be compared to the observed ones, shown in Fig. 6.

The results of this procedure are shown in Fig. 8. This figure demonstrates that the derived LFs can be fitted much better to the equation (2) than previously. We get $M_I^{\rm max} = -0.149$, $\sigma = 0.167$ for all clump stars, $M_I^{\rm max} = -0.148$, $\sigma = 0.137$ for the red ones, and $M_I^{\rm max} = -0.149$, $\sigma = 0.22$ for the blue ones. Clearly, the σ-values are close to the observed ones obtained in the previous section (and Fig. 6). $M_I^{\rm max}$ for the whole sample and the red colour bin are not influenced by the convolution. However, particularly interesting is that the faint wing of the LF for the blue sample (at $0.3 > M_I > -0.1$ in the lower panel of Fig. 7), after the convolution, becomes indistinguishable from the main body of the clump. In this case, the fitting routine includes those fainter stars into the gaussian curve. Therefore, a fainter $M_I^{\rm max}$ is obtained for the blue stars. The $M_I^{\rm max}$ difference between blue and red stars becomes null due to this effect.

Moreover, this theoretical red clump LF shares several characteristics with the observed one: very nice gaussian profiles for the central clump; the presence of extended wings which end at about $M_I = 0.8$ at the faint side, and at $M_I = -1.8$ in the bright one; comparable values of σ and $M_I^{\rm max}$; a larger σ for the blue stars; and, most important, $M_I^{\rm max}$ values almost independent of $V - I$. This latter characteristic is essentially due to the fact that the stars at the bluest extreme of the red clump are of higher masses, thus being on the mean younger and fainter than the remaining clump stars. As they are, in general, not clearly separated in M_I from the main red clump (especially for the sample with < 10% parallax errors), they have a weight in determining the mean clump magnitude $M_I^{\rm max}$. How much $M_I^{\rm max}$ can be affected by the young stars, however, depends essentially on two factors:

1. On the relative proportion of young (ages around 1 Gyr) to old (> 1 Gyr) stars. Comparison of Figs. 8 and 6 reveals that the simulation with constant star formation rate provides almost the same relative number of stars in the red and blue parts of the clump as in the *Hipparcos* sample. This could suggest that the star formation rate 1 Gyr ago was the same as the mean over the Galactic Disk history. Of course, any conclusion of this kind requires closer scrutiny by means of more realistic models for the age-metallicity relation, initial mass function, and scale heights of different stars, which is beyond the scope of this paper.
2. Whether these stars fall inside or outside the colour interval defined to measure $M_I^{\rm max}$. In the case of *Hipparcos* data, the complete red clump falls in the $0.8 < (V-I) < 1.25$ interval used to define the reference $M_I^{\rm max}$ by Pacziński & Stanek (1988). In the case of stellar populations with a lower mean metallicity as the Magellanic Clouds, the red clump is observed at much bluer colours, and falls partially out of the $0.8 < (V-I) < 1.25$ interval. For instance, Fig. 2 in Stanek et al. (1998) shows that the red clump in the LMC ranges from $V-I = 0.6$ to 0.9. In this case, only the reddest tail of the clump falls inside $0.8 < (V-I) < 1.25$, which probably excludes the younger (and fainter) stars from their estimate of $I^{\rm max}$ for this galaxy.

Both factors mean that there can be systematic effects in the $I^{\rm max}$ measurement, that are determined by the way we sample the clump stars and by the relative contribution of young stars to the composite stellar population observed.

Our models reproduce the fact that $M_I^{\rm max}$ is almost constant over the $V-I$ interval considered in the case of *Hipparcos* data, and yet predict a significant dependence of the clump magnitudes with metallicity (Fig. 1). This is mainly due to the dependence of the underlying stellar models' luminosity on metallicity. For the transformation into M_I, we only have to assume that the bolometric corrections given by Kurucz (1992) have the correct (weak) dependence on metallicity.

5. The expected $M_I^{\rm max}$ for the LMC

The history of star formation in the LMC has been intensively studied in the last years (Bertelli et al. 1992; Vallenari et al. 1996; Gallagher et al. 1996; Holtzman et al. 1997; Elson, Gilmore & Santiago 1997; Stappers et al. 1997), by means of CMDs of different fields. Most of these works point out that the star formation rate in the LMC was higher in the last few Gyr than in the interval from about 3 to ~ 12 Gyr. That is in agreement with the fact that no cluster is known with ages in the $4-10$ Gyr interval (van den Bergh 1981; Da Costa 1991; Girardi et al. 1995; Olzsewski, Suntzeff & Mateo 1996; Geisler et al. 1997). Elson et al. (1997) present additional evidences that a later burst of stellar formation has taken place about 1 Gyr ago, while Geha et al. (1998) propose that a continuous stellar formation history was followed by an enhancement of star formation from 2 Gyr to now.

With respect to the abundances of LMC stars, the results from CMD studies are not conclusive in giving a clear age-metallicity relation for the LMC. This applies also to clusters: while Olszewski et al. (1991) pointed out that intermediate-age LMC clusters have a mean $[{\rm Fe/H}] = -0.4$ (or $Z = 0.008$), there are several claims in the literature that a significantly lower value would be more appropriate (see Bica et al. 1998, and references therein).

Given the variety of solutions suggested by several authors, we prefer to limit our analysis to two scenarios. For them, Fig. 9 shows the derived stellar density in the M_I vs. $V-I$ plane, compared to that meant to represent *Hipparcos* data. The first one assumes simply a constant star formation rate between ages 0.1 and 3 Gyr, with metallicities equally probable between $Z = 0.004$ and 0.008. This model provides a clump with some structure, especially in its blue part, and located at the border of the $0.8 < (V-I) < 1.25$ interval (again, if a $\Delta(V-I) = -0.07$ shift is previously applied to the models). Following the suggestion by Cole (1998), we tested a second scenario similar to that of Vallenari et al. (1996): 44% of the clump being produced by $[0.006 < Z < 0.010,\ 0.1 < (t/{\rm Gyr}) < 2]$ populations, the remaining 56% by $[0.002 < Z < 0.006,\ 2 < (t/{\rm Gyr}) < 10]$ ones. Indeed, this alternative provides a model more similar to the apparently featureless clump observed by Stanek et al. (1998). The scenario proposed by Holtzman et al. (1997), instead, would produce a clump separated into a blue [with $Z = 0.001$ and $2 < (t/{\rm Gyr}) < 10$] and a red [with $Z = 0.008$ and $1 < (t/{\rm Gyr}) < 2$] component, contrary to observations; therefore we preferred not to test this possibility here.

As simple as these simulations are, they indicate a clump located about 0.2 mag to the blue in $V-I$, and about 0.2 mag brighter in M_I than the local one sampled by *Hipparcos*. Comparison of this clump with the observed one presented by Stanek et al. (1988) is not conclusive. In fact, their data show a featureless clump, about 0.3 mag wide in $V-I$ and with a $\sigma(I)$ of about 0.15 mag. Part of this width can be attributed to the dispersion in reddening in the observed fields. The standard errors in the determination of the mean E_{V-I} and A_I by Stanek et al. (1998),

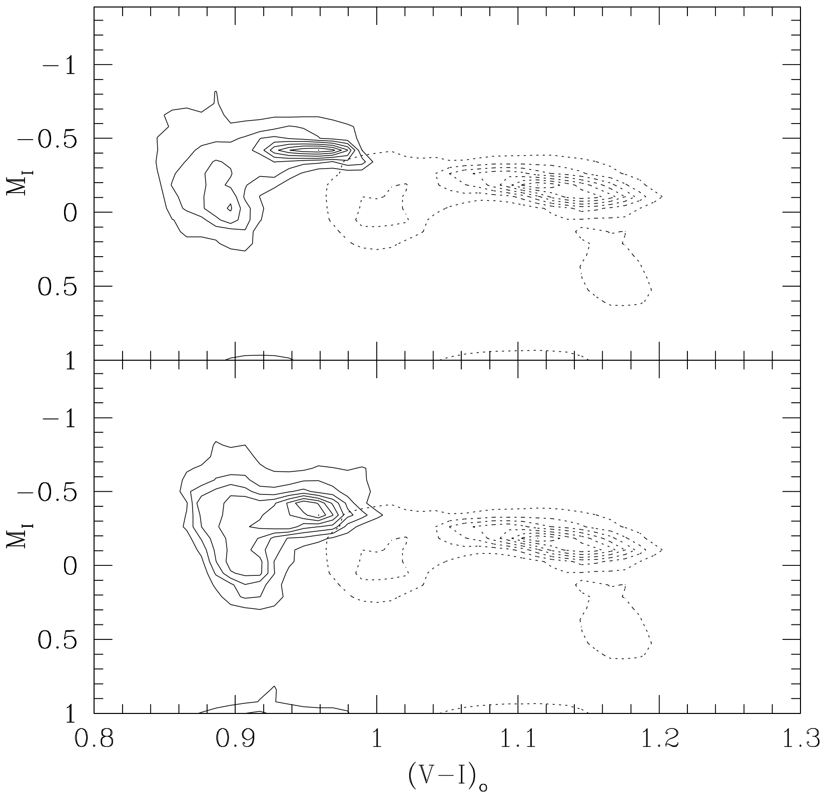

Fig. 9. Theoretical density of stars in the M_I vs. $V-I$ diagram, for the models meant to represent the LMC data (continuous lines). For the sake of comparison, the model for the *Hipparcos* data (Fig. 2) is also repeated (dotted lines). Only the contour levels corresponding to the red clump are shown. Upper panel: model with $[0.004 < Z < 0.008, 0.1 < (t/\mathrm{Gyr}) < 3]$; lower panel: model with a star formation and chemical enrichment history similar to that suggested by Vallenari et al. (1997; see text for details).

$\sigma(E_{V-I}) = 0.05$ and $\sigma(A_I) = 0.08$, represent a lower limit to the magnitude of this dispersion. Models in Fig. 9 do not include these effects. Moreover, we remark that attempts to derive the best clump model should better take into account the distribution of stars in the complete CMD, and not only in the clump, in order to constrain the possible solutions. Again, this is beyond the scope of this paper.

The LF for these theoretically predicted clumps are presented in Fig. 10. Fits to these curves according to equation (2) produce values of $M_I^{\rm max} = -0.384$, $\sigma = 0.043$ for the simple simulation, and $M_I^{\rm max} = -0.326$, $\sigma = 0.097$ for the complex one. The latter is wider and fainter than the former, since the lowest-luminosity stars of the clump are in this case partially included in the colour bin used to compute the LF. In any case, the $M_I^{\rm max}$ values are $0.17 - 0.23$ mag brighter than than those predicted for local stars. The dispersion $\sigma = 0.089$ can be compared the $\sigma = 0.15$ value found for LMC data by Udalski et al. (1998) and Stanek et al. (1998). It accounts for 2/3 of the observed value, which, as above remarked, should include a dispersion in A_I of at least 0.08 mag.

Which one of the above values of $M_I^{\rm max}$ should be preferred, is open to discussion. In the case of Stanek et al.'s (1998) work, it is clear that they sampled only the very red extremity of the clump in order to define $I^{\rm max}$. This case would better correspond to the $M_I^{\rm max} = -0.384$ case in our simulations.

If we take this latter simulation as a reference, we conclude that the $M_I^{\rm max}$ value for the LMC should be lower by about $\Delta M_I^{\rm max} = -0.235$ mag with respect to the value obtained by simulating the local clump (as shown in Fig. 8). If we take at face value the mean $I_0^{\rm max} = 17.835 \pm 0.008$ value obtained by Stanek et al. (1998) for the LMC, and the reference value of $M_I^{\rm max} = -0.209$ measured by *Hipparcos* data corrected for Lutz-Kelker bias, we then derive a

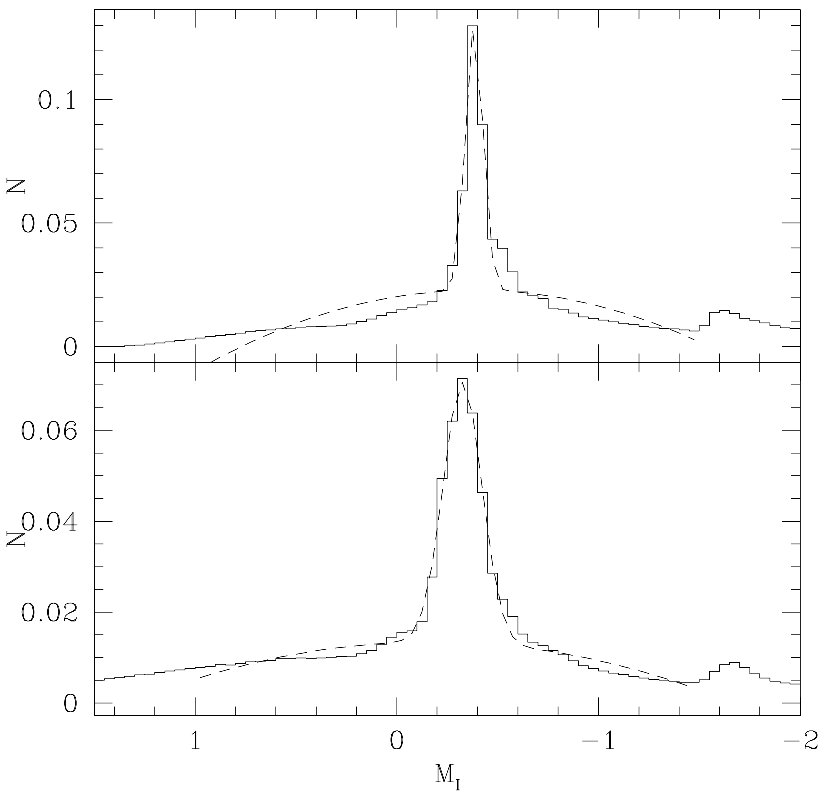

Fig. 10. Theoretical LFs for the LMC models (solid lines), together with the fit of equation (2) (dashed lines). Upper and lower panels correspond to those of Fig. 9.

distance to this galaxy of $(m-M)_0 = I_0^{\rm max} - M_I^{\rm max} - \Delta(M_I^{\rm max}) = 18.279$. Uncertainties, however, are not simply given by the uncertainty in photometry. $\Delta M_I^{\rm max}$ values are model-dependent, and the numbers here used may be regarded as a simple, first-order estimate for this quantity, uncertain to about 0.1 mag. Intrinsic errors in the $M_I^{\rm max}$ determination and in reddening (Udalski et al. 1998; Stanek et al. 1998) would add a 0.15 mag uncertainty to these numbers.

Our conclusion, then, is that from this first simulation of the local and LMC clump, the LMC should be located farther away by $\Delta(m-M)_0 = +0.23$ mag with respect to the values obtained by Udalski et al. (1998) and Stanek et al. (1998). This result is in qualitative agreement with that obtained by Cole (1998), who from simple considerations about the age and metallicity differences between local and LMC stars adopted a correction of $\Delta(m-M)_0 = +0.32$ mag. Our results are characterised by the use of more complex models, which recover many of the details of the clump defined by *Hipparcos*.

The LMC distance determination of 18.28 ± 0.18 mag is compatible with the generally accepted value of about 18.5 ± 0.1 mag, found by means of several different methods over the last years (e.g. Westerlund 1990; Panagia et al. 1991; Madore & Freedman 1998; Salaris & Cassisi 1998; Oudmaijer, Groenewegen & Schrijver 1998).

Our results can by no means be considered as a firm determination of the LMC distance with the red giant clump method, because there remain many uncertainties in the population syntheses to be solved, as there are the mentioned assumptions about the age-metallicity-relation and star formation history.

These uncertainties are absent for a population of single-aged stars of identical composition as is present in globular clusters. Therefore, we applied our method for testing purposes to the galactic metal-rich disk cluster 47 Tuc. Kaluzny et al. (1998) determine the extinction-corrected clump magnitude as $I_0^{\rm max} = 13.109 \pm 0.026$. Using the *Hipparcos*-clump brightness as a standard candle, they obtain a distance modulus of $(m-M)_0 = 13.34$. Our models, using a solar-scaled isochrone of 10 Gyr with $Z = 0.01$ and $Y = 0.25$ predict $M_I^{\rm max} = -0.13$, with a dispersion of only 0.014 mag, confirming the observed narrow brightness peak. (An additional dispersion can be obtained if higher mass loss is assumed.) However, this value for $M_I^{\rm max}$ has to be corrected for two chemical pecularities: first, 47 Tuc shows α-element enhancement. Salaris & Weiss (1998) showed that this leads to core helium-burning models being 0.15 mag brighter than solar-scaled ones at the same total metallicity. Second, Salaris & Weiss (1998) argue strongly that the helium content in 47 Tuc is close the solar value of ≈ 0.27, which again leads to brighter models (-0.05 mag), such that the distance from the clump model is modified to $(m-M)_0 = 13.44$. For comparison, Salaris & Weiss (1998), who determined the age of 47 Tuc to 9.2 ± 1.1 Gyr, obtain 13.38 ± 0.05 from ZAHB models. Within the uncertainties, this number agrees with both the empirical and the theoretical clump distance. The larger difference between the latter two values can be explained by the fact that 47 Tuc has a lower metallicity than the average local clump star and therefore is farther away than the standard-candle assumption of Kaluzny et al. (1998) would predict. To close this discussion about 47 Tuc, Gratton et al. (1997) from *Hipparcos* subdwarf fitting find $(m-M)_0 = 13.50$ and Reid (1998) with similar data and method 13.57. Of all values listed above, our clump distance agrees best with these completely independent results.

Another source of error might be the transformations from theoretical to observed quantities. We find, however, that our results change just little if we use different tables of bolometric corrections. For instance, the I bolometric corrections derived from Yale tables (Green 1988) have a slightly lower dependence on metallicity than those from Kurucz (1992). The use of these tables would cause an additional change of about $\Delta(m-M)_0 = -0.04$ mag in the LMC distance modulus.

A further potential source of uncertainty is the dependence of $M_I^{\rm max}$ with the helium content. Only to give an idea of the possible effects, a change of $\Delta Y = +0.01$ would cause clump models of a given mass and Z to have clump magnitudes lower (i.e. brighter) by -0.04 mag. Of course, any of the theoretical predictions about the mean clump magnitude, depend on the assumption that Y increases with Z according to a known $Y(Z)$ relation. The relation adopted here represents a quite conservative one, since present-day observations (see e.g. the discussion in Pagel & Portinari 1998) are not able to constrain the $\mathrm{d}Y/\mathrm{d}Z$ ratio to the accuracy which would be desirable in this kind of study.

6. Final comments

In this work we discuss the morphology of the red clump in composite stellar populations and the possible origin of systematic errors in the method of distance determination by means of these stars. These systematic effects are such that $M_I^{\rm max}$ depends only weakly on the $V-I$ colour for a galaxy population (as the sample observed by *Hipparcos*), but is systematically brighter for lower values of the mean galaxy metallicity. This explains the low distance modulus obtained for the LMC under the assumption that $M_I^{\rm max}$ is independent of age and metallicity (Udalski et al. 1998; Stanek et al. 1998), and provides a value closer to the traditional one when the metallicity and age dependence suggested by present models is considered. This method of distance determinations should therefore be used with care in galaxies where the history of stellar formation and chemical enrichment has been very different from the local galactic disk, as is the case for the Magellanic Clouds.

Our results also help to understand why the distance to M31 obtained by means of this method (Stanek & Garnavich 1998) is in agreement with that obtained by other independent methods: it probably reflects the fact that the mixture of stellar populations in the red clump of M31 [defined however in the $0.8 < (V-I) < 1.25$ colour interval] is similar to the local disk one. The red clump method, in this particular case, may work well with the assumption that the $M_I^{\rm max}$ determined from *Hipparcos* data could be compared to $I^{\rm max}$ observed in this galaxy.

Also in the case of galactic bulge stars, it may well be that the distance determination by Paczyński & Stanek (1998) do not suffer from significant systematic errors. This is for a different and more subtle reason: In the case of stellar populations with metallicities from approximately solar to twice solar (as for the bulge), the trend of increasing $M_I^{\rm max}$ with metallicity can be reversed if the helium content increases proportionally with Z. It causes $M_I^{\rm max}$ to be less sensitive to metallicity than for more metal-poor populations. Such an effect can be appreciated by comparing the $Z = 0.019$ and 0.03 models in Fig. 1. In this Z interval, models of similar age differ significantly in $V-I$ colour, but not in absolute magnitude. This would support the assumption that $M_I^{\rm max}$ in Baade's Window stars is similar to that given by *Hipparcos*, and would also explain the absence on any trend in $I^{\rm max}$ with colour for them (Paczyński & Stanek 1998).

On the other hand, the quest for a main revision of the calibration of the extragalactic distance scale, that would be suggested by a short distance to the LMC, is significantly weakened by the present results. Indeed, they show that red clump stars cannot be considered as standard candles. The assumption that $M_I^{\rm max}$ is independent of the stellar population can provide distance determinations accurate to only about 0.5 mag. Lower uncertainties are expected only in the case we have additional information about the history of stellar formation and metal enrichment of the galaxy to which the method is applied. Therefore, this method of distance determination does not improve over others currently used.

Another point of concern raised by the present work regards the stellar models of clump stars. The fine structure observed in the blue part of the red clump reflects directly the dependence of the core mass at He ignition on the initial stellar mass. Our models successfully predict this structure only because this dependence is implicitly taken into account in all evolutionary sequences we computed. However, models of red clump and horizontal branch stars have often been computed under the assumption that the core mass at He ignition is constant for all low-mass stars; this approximation has been necessary because computing tracks up to the RGB tip is rather time-consuming. Results of such calculations have been used by Cole (1998), for instance. However, given the present results and the quality of photometric data to come, such a simplification can no longer be justified when the objective is the interpretation of the red clump in composite stellar populations. Also, grids of evolutionary tracks with mass resolution of 0.1 $M_{\odot}$ as here adopted, or even lower, may be desirable in order to produce realistic models of the red clump.

Acknowledgments

Thanks are due to Y.K. Ng and P. Marigo for their useful comments, and to B. Paczyński for the debate which stimulated this work. We made use of the Simbad database, mantained by the CDS, Strasbourg. The work by L. Girardi is funded by the Alexander von Humboldt-Stiftung.

References

Beaulieu J.-P., Sackett P.D., 1998, AJ in press (astro-ph/9710156)
Bertelli G., Bressan A., Chiosi C., 1985, A&A 150, 33
Bertelli G., Mateo M., Chiosi C., Bressan A., 1992, ApJ 388, 400
Bertelli G., Bressan A., Chiosi C., Fagotto F, Nasi E., 1994, A&AS, 106, 275
Bica E., Geisler D., Dottori H., Clariá J.J., Piatti A.E., Santos Jr. J.F.C., 1998, AJ in press (astro-ph/9803167)
Buonanno R., Corsi C.E., Fusi Pecci F., 1985, A&A 145, 97
Carraro G., Ng Y.K., Portinari L., 1998, MNRAS in press (astro-ph/9707185)
Cassisi S., Salaris M., 1997, MNRAS 285, 593
Charlot S., Worthey G., Bressan A., 1996, ApJ 457, 625
Chiosi C., Bertelli G., Bressan A., 1992, ARA&A 30, 235
Cole A.A., 1998, ApJ in press (astro-ph/9804110)
Corsi C.E., Buonanno R., Fusi Pecci F., Ferraro F.R., Testa V., Greggio L., 1994, MNRAS 271, 385
Da Costa G., 1991, in IAU Symp. 148, The Magellanic Clouds, eds. Haynes R., Milne D., Dordrecht: Kluwer, p. 183
Edwards T.W., 1976, AJ 81,245
Elson R.W., Gilmore G.F., Santiago B.X., 1997, MNRAS 298, 157
ESA, 1997, 'The Hipparcos and Tycho Catalogues', ESA SP-1200
Fusi Pecci F., Ferraro F.R., Crocker D.A., Rood R.T, Buonanno R., 1990, A&A 238, 95
Gallagher J.S., Mould J.R., De Feijter E., et al., 1996, ApJ 466, 732
Geisler D., Bica E., Dottori H., Clariá J.J., Piatti A.E., Santos Jr. J.F.C., 1997, AJ 114, 1920
Geha M.C., Holtzman J.A., Mould J.R., et al., 1998, (astro-ph/9711144)
Girardi L., Chiosi C., Bertelli G., Bressan A., 1995, A&A 298, 87
Girardi L., Bressan A., Chiosi C., 1996, in Stellar Evolution: What Should Be Done, 32nd Liège Int. Astrophys. Coll., eds. A. Noels et al., p. 39.
Girardi L., Bertelli G., 1998, MNRAS submitted (astro-ph/9801145)
Girardi L., Bressan A., Bertelli G., 1998, in preparation
Gratton R., Carretta E., Castelli F., 1996, A&A 314, 191
Gratton R., Fusi Pecci F., Carretta E., et al., 1997, ApJ 491, 749
Green E.M., 1988, in Calibration of stellar ages, ed. A.G. Davis Philip, L. Davis Press, p. 81
Heintz W.D., 1982, PASP 94, 705
Heintz W.D., 1986, A&AS 65, 411
Holtzman J.A., Mould J.R., Gallagher J.S., et al., 1997, AJ 113, 656
Jimenez R., Flynn C., Kotoneva E., 1998, MNRAS submitted (astro-ph/9709056)
Kaluzny J., Wysocka A., Stanek K.Z., Krzemiński W., 1998, in preparation
Kurucz R.L., 1992, in The Stellar Populations of Galaxies, eds. B. Barbuy and A. Renzini, Dordrecht: Kluwer, p. 225
Lutz T.E., Kelker D.H., 1973, PASP 85, 573
Maeder A., Meynet G., 1989, A&A 1989 210, 155
Madore B.F., Freedman W.L., 1998, ApJ 492, 110
Olive K., Steigman G., ApJS 97, 49

Olszewski E.W, Schommer R.A., Suntzeff N.B., Harris H.C., 1991, AJ 101, 515
Olszewski E.W, Suntzeff N.B., Mateo M., 1996, ARA&A 34, 511
Oudmaijer R.D., Groenewegen M.A.T., Schrijver H., 1998, MNRAS 294, L41
Panagia N. Gilmozzi R., Macchetto F., Adorf H.M., Kirschner R.P., 1991, ApJ 380, L23
Pagel B.E.J., Portinari L., 1998, MNRAS in press, (astro-ph/9711332)
Perryman M.A.C., et al., 1997, A&A 323, L49
Paczyński B., Stanek K.Z., 1998, ApJ 494, L219
Reimers D., 1975, Mem. Soc. R. Sci. Liège, ser. 6, vol. 8, p. 369
Renzini A., 1977, in Advanced stages in stellar evolution, eds. Bouvier P., Maeder A., Geneva Obs., p. 149
Renzini A., Buzzoni A., 1986, in Spectral Evolution of Galaxies, eds. C. Chiosi and A. Renzini, Dordrecht: Reidel, p. 195
Renzini A., Fusi Pecci F., 1988, ARA&A 26, 199
Salaris M., Cassisi S., 1998, MNRAS in press (astro-ph/9803103)
Salaris M., Groenewegen M.A.T., 1998, MNRAS, submitted
Salaris M., Weiss A., 1998, A&A, accepted
Seidel E., Demarque P., Weinberg D., 1987, ApJS 63, 917
Smith H. Jr., 1987, A&A 188, 233
Sommer-Larsen J., 1991, MNRAS 249, 368
Stanek K.Z., Zaritsky D., Harris J., 1998, (astro-ph/9803181)
Stanek K.Z., Garnavich P.M., 1998, ApJ in press (astro-ph/9802121)
Stappers B.W., Mould J.R., Sebo K.M., et al., 1997, PASP 109, 292
Stephenson C.B., Sanwal N.B., 1969, AJ 74, 689
Sweigart A.V., Gross P.G., 1976, ApJS 32, 367
Sweigart A.V., Greggio L., Renzini A., 1990, ApJ 364, 527
Torres-Peimbert S., Peimbert M., Fierro J., 1989, ApJ 345, 186
Turon Lacarrieu C., Crézé M., 1977, A&A 56, 273
Udalski A., Szymański M., Kubiak M., Pietrzyński G., Woźniak P., Żebruń K, 1998, AcA 48, 1
Vallenari A., Chiosi C., Bertelli G., Aparicio A., Ortolani S., 1996 A&A 309, 367
van den Bergh S., 1981, A&AS 46, 79
Westerlund B.E., 1990, A&AR 2, 29
Worley C.E., Heintz W.D., 1983, The fourth catalog of orbits of visual binary stars, Pub. U.S. Naval Obs. 2nd Serie, 24, 1
Worley C.E., Douglass G.G., 1997, The Washington Double Star Catalog, A&AS 125, 523
Worthey G., 1994, ApJS, 95, 107
Zaritski D., Lin D.N.C, 1997, AJ 114, 2545

A. Consideration of *Hipparcos* parallax errors in the LF

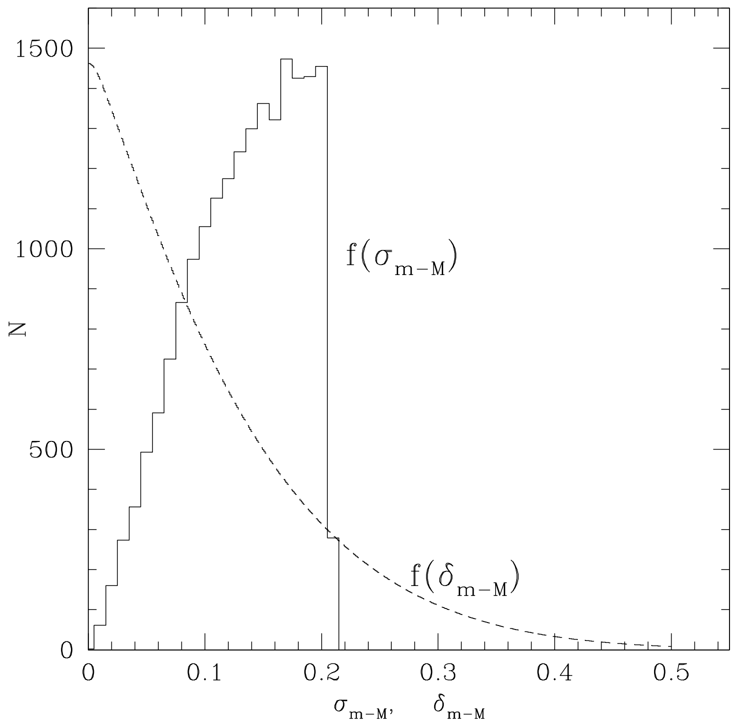

Fig. 11. Distribution of standard errors in distance modulus, $f(\sigma_{m\text{–}M})$ for the stars in *Hipparcos* catalog with parallax errors smaller than 10% (continuous line). Assuming that errors in $m-M$ are gaussian functions, the probability of having a $m-M$ error of $\delta_{m\text{–}M}$ is given by the dashed line.

In Section 4.2 it was argued that the theoretical LF for the local clump has to be convolved with the error distribution of *Hipparcos* parallaxes in order to allow a realistic comparison with observed data. Fig. 11 shows the distribution of standard errors in distance modulus for the 19143 stars with parallax known to better than 10% in *Hipparcos* catalog (using also additional quality criteria similar to those defined in Section 3.2), or $f(\sigma_{m\text{–}M})$. A very similar distribution of errors is obtained if we limit the sample to the clump stars. The mean error in distance modulus for the complete sample is $\langle\sigma_{m\text{–}M}\rangle = 0.134$.

In order to simulate the effect of distance errors in our simulation, we should convolve the theoretical LFs by a sample of gaussian curves, each one of standard deviation $\sigma_{m\text{–}M}$, representing the complete distribution of $\sigma_{m\text{–}M}$ values observed in the sample of *Hipparcos* data. The resulting distribution of absolute errors, $f(\delta_{m\text{–}M})$, is given by

$$f(\delta_{m\text{–}M}) = \int_0^{{\sigma_{m\text{–}M}}^{\max}} \frac{f(\sigma_{m\text{–}M})}{\sigma_{m\text{–}M}\sqrt{2\pi}} \times \exp\left[-\frac{(m-M)^2}{2{\sigma_{m\text{–}M}}^2}\right] \mathrm{d}\sigma_{m\text{–}M} \; , \qquad \text{(A1)}$$

This function is also depicted in Fig. 11 (only for $\delta_{m\text{–}M} > 0$). It includes the complete spectrum of distance errors expected to be in the sample limited to 10% parallax (standard) errors. An important point to be noticed is that this function is already wider than the width of the theoretical distributions we have, which have typically $\sigma \simeq 0.08$ mag.

This article was processed by the author using a modified version of the Springer-Verlag LaTeX A&A style file *L-AA* version 3.